Journal of Electrical Engineering & Technology (2020) 15:2501–2508
https://doi.org/10.1007/s42835-020-00534-2

ORIGINAL ARTICLE

Magnetization Characteristics Due to Fault Angle of Transformer Type SFCL with Two Isolated Secondary Windings

Tae-Hee Han[1] · Sung-Hun Lim[2] · Seok-Cheol Ko[3]

Received: 4 March 2020 / Revised: 9 June 2020 / Accepted: 28 August 2020 / Published online: 8 September 2020

Abstract
In this paper, a transformer type superconducting fault current limiter (SFCL) with two isolated secondary windings was fabricated to increase the current limiting capacity. As the magnetization current increased due to the large transient fault current immediately after the fault, the magnetization force variation, the operating range of the flux linkage, and the voltage region variation were compared at fault angles of 0° and 90°, respectively. The short-circuit test analyzed the current limiting operation, power consumption, and energy consumption characteristics according to the fault angle immediately after the fault occurrence. The results showed that the fault angle of 0° could limit the fault current much more than the fault angle of 90°. In addition, it was confirmed that the magnetization force variation, the operating range of the flux linkage, and the voltage induced in the primary winding were all much larger at the fault angle of 0° than at the fault angle of 90°.

Keywords Fault angle · Isolated secondary windings · Magnetization current · Magnetization force variation · Superconducting fault current limiter (SFCL) · Transformer type

1 Introduction

Short circuit accidents occur frequently in power systems for a number of reasons, and superconducting fault current limiters (SFCLs) are the most commonly used devices to prevent them [1–3]. Under normal operating conditions, the SFCL is the ideal device for limiting fault current in the event of a short circuit due to near-zero impedance and fast steady state transitions. To date, the characteristics of various types of SFCLs such as resistive type, saturated iron-core type, magnetic shield type, bridge type, active and high-speed switching type, inductive and hybrid type, transformer type, flux-lock type, and flux-coupling type have been studied [4–14]. When a large fault current occurs, the superconducting element has to bear the fault current detection and the limiting operation at the same time, which is a burden for the superconducting element. As a way to increase the current limiting capacity, studies on the current limiting characteristics of the hybrid type SFCL, in which a superconducting element is connected in series or in parallel, have been carried out [15–18]. In addition, the peak current limiting characteristics of a transformer type SFCL with additional coupling circuits and a transformer type SFCL with two non-isolated secondary windings were compared in different wiring directions [19, 20]. However, the characteristics such as magnetization and power consumption according to the fault angle have not been investigated during the fault period. In the transformer type SFCL using superconducting elements, it can be considered that the magnetization characteristics analysis is very important because it is related to the AC loss. Due to the fault current of the line, the resistance caused by the quench occurs in the superconducting element, and the magnetic flux is no longer canceled out, and the voltage is induced in the secondary winding, thereby increasing the limiting impedance value to

✉ Seok-Cheol Ko
suntrac@kongju.ac.kr

Tae-Hee Han
hantaehee@jwu.ac.kr

Sung-Hun Lim
superlsh73@ssu.ac.kr

[1] Department of Aero Materials Engineering, Jungwon University, Goesan, Chungbuk, Republic of Korea

[2] Department of Electrical Engineering, Soongsil University, Seoul, Republic of Korea

[3] Industry-University Cooperation Foundation and Regional-Industrial Application Research Institute, Kongju National University, Gongju, Chungnam, Republic of Korea

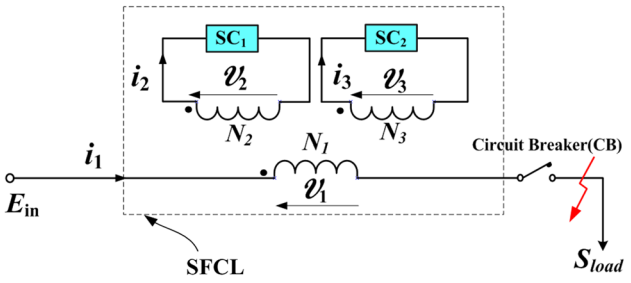

Fig. 1 Schematic configuration of a transformer type SFCL with two isolated secondary windings, which are subtractive polarity winding

limit the fault current. The purpose of this study is to analyze the magnetization characteristics, such as the change in the flux linkage and the magnetization force in each device due to the magnetizing current.

In this paper, to increase the current limiting capacity, as shown in Fig. 1, the magnetization characteristics of a transformer type SFCL insulated from secondary and tertiary windings in the secondary side of the transformer are compared at fault angles of 0° and 90°. The magnetization current (I_m) and limiting impedance (Z_{SFCL}) equations of a transformer type SFCL with two isolated secondary windings were derived from the electrical equivalent circuit. Through a short-circuit experiment, we compared the double peak current limiting operation, voltage waveform, instantaneous power, and magnetic flux of each device based on the fault angle immediately after the fault occurrence. In addition, we compared the change in the magnetization force region, the operating range of the flux linkage, and the primary voltage variation region due to the influence of the magnetization current. Laboratory scale prototypes were fabricated, and fault tests were performed. The purpose of this study was to verify the usefulness of the fault current limiting operation and magnetization characteristics by double quench.

2 Structure and Operating Principle

2.1 Structure and Operating Principle

Figure 1 shows the structure of the transformer type SFCL with two isolated secondary windings. The high- temperature superconducting elements (SC_1 and SC_2) are connected to the secondary winding and the tertiary winding through the ferromagnetic iron core. The direction of wiring between the primary winding and the secondary and tertiary windings is the subtractive polarity winding. The high-temperature superconducting (HTSC) elements used a $Y_1Ba_2Cu_3O_{7-x}$ (YBCO) thin film deposited with a 200 nm thick platinum layer manufactured by Theva (Germany) with a critical temperature of 87 K.

The basic operating principle of the transformer type SFCL with two insulated secondary windings is that zero voltage appears in superconducting elements because SC_1 and SC_2 maintain zero resistance under normal conductions. If a fault current (i_1) occurs due to a ground fault or short circuit, a resistance (R_{sc1}) is generated in the superconducting element SC_1 connected to the secondary winding, which limits some of the fault current. At this time, when part of the fault current does not exceed the critical current (I_C) of the superconducting element SC_2, which is the second peak current limiting element, the superconducting element SC_1 maintains zero resistance, and the fault current (i_1) is limited only by R_{sc1}. However, if a large fault current occurs, the critical current (I_C) of the superconducting element SC_2 constituting the second peak current limiting element is exceeded, and resistance (R_{sc2}) of the superconducting element SC_2 connected to the tertiary winding is additionally generated. Therefore, the fault current is limited by R_{sc1} and R_{sc2}.

2.2 Equivalent Circuit

Figure 2 shows the electrical equivalent circuit of the transformer type SFCL with two isolated secondary windings. Electrical equivalent circuits can be derived from magnetic equivalent circuits using the topology principle of duality [21]. The resistance and leakage inductance of each winding are omitted for simplicity. L_1 and L_{Th} represent the self-inductance wound on the primary side of the ferromagnetic iron core and the equivalent inductance for the primary and two secondary windings, respectively. From the equivalent circuit of the transformer type SFCL, the magnetization current (I_m) and the limiting impedance (Z_{SFCL}) can be expressed by Eqs. (1) and (2), respectively:

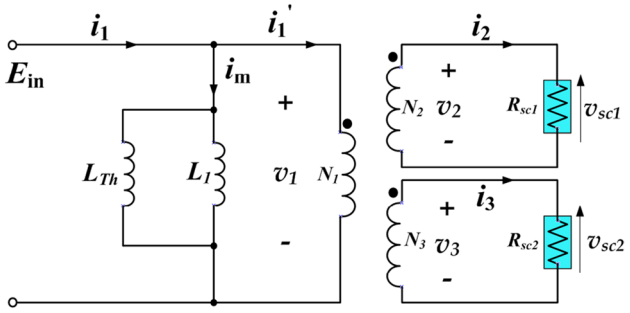

Fig. 2 Electrical equivalent circuit of the transformer type SFCL with two isolated secondary windings

$$I_m = I_1 - \left(\frac{N_2}{N_1} I_2 + \frac{N_3}{N_1} I_3\right) \tag{1}$$

$$Z_{SFCL} = 1 \Big/ \left[\frac{1}{V_1}\left(\frac{N_2}{N_1}\frac{V_{SC1}}{R_{SC1}} + \frac{N_3}{N_1}\frac{V_{SC2}}{R_{SC2}}\right) + \frac{1}{j\omega L_{eq}}\right] \tag{2}$$

Here, V_1, V_2, V_{SC1}, and V_{SC2} in phasor form are the voltages induced in the primary and secondary windings and the superconducting elements (SC_1 and SC_2), respectively. N_1, N_2, and N_3 represent the turns of each winding, and L_{eq} is equal to L_{Th} // L_1. *Rsc1* and *Rsc2* represent the resistances of the superconducting elements SC_1 and SC_2, respectively, and ω represents each frequency.

The design parameters of the two isolated transformer type SFCLs are shown in Table 1. The direction of connection between the primary winding and the two secondary windings is the subtractive polarity winding, and it is designed to compare and analyze the magnetization characteristics based on fault angles of 0° and 90°.

3 Experimental Results

3.1 Preparation of Experiment

Figure 3 shows the experimental configuration for the short-circuit test of the transformer type SFCL with two insulated secondary windings. It consists of a 200 V AC supply voltage (E_{in}) at 60 Hz, a line reactance (X_{line}) of 0.69 Ω, a line resistance (R_{line}) of 0.097 Ω, a load resistance (R_{load}) of 41.2 Ω, and a transformer type SFCL. In order to simulate a short- circuit accident, SW_1 was turned on in the first step. In the second step, SW_2 was turned on to cause a short-circuit accident. After five cycles, SW_2 was opened again to eliminate the fault occurrence. During the fault period, the currents and voltages flowing through each winding and the superconducting elements were measured by a current transformer (CT) and a potential transformer (PT), respectively.

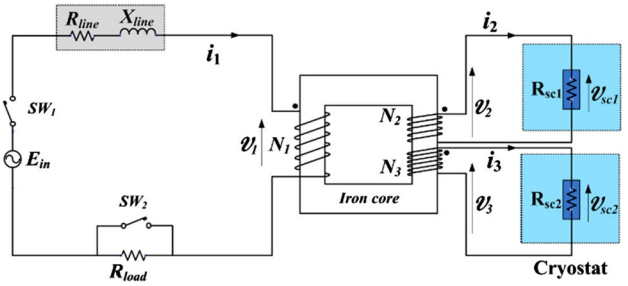

Fig. 3 Experimental circuit for the short-circuit test of the transformer type SFCL with two isolated secondary windings

3.2 Experimental Results

Figure 4(a) shows the operating characteristics of the voltage and current of each winding and superconducting element at a fault angle 0°. When the fault occurs, the voltage is shown to proportionally depend on the number of turns of each winding. In the case when the fault current is large, the quench occurs in superconducting elements SC_1 and SC_2, which constitutes the first and second limiting elements, and the voltage of these superconducting elements occurs in proportion to the number of turns. When the fault occurs, the total current of SFCL rapidly increases in the beginning, but it can be seen that the total current is small during the five cycles of fault. It also can be seen that the fault current is limited by the quench of superconducting elements SC_1 and SC_2 constituting the first and second limiting elements. During the fault period, it can be observed that the magnetization current is larger at the fault angle of 0° than at the fault angle of 90°.

Figure 4(b) shows the operating characteristics of the voltage and current of each winding and superconducting element at the fault angle of 90°. When the fault occurs, the fault current is small, and it can be seen that the quench

Table 1 Specifications of the transformer type SFCL with two isolated secondary windings

Primary and two secondary windings	Value	Unit
Primary winding (N_1)	60	Turns
First secondary winding (N_2)	15	Turns
Second secondary winding (N_3)	75	Turns
Two HTSC elements (SC_1 and SC_2)	Value	Unit
Material	YBCO	
Fabrication form	Thin Flim	
Critical temperature (T_c)	87	K
Critical current (I_c)	27	A

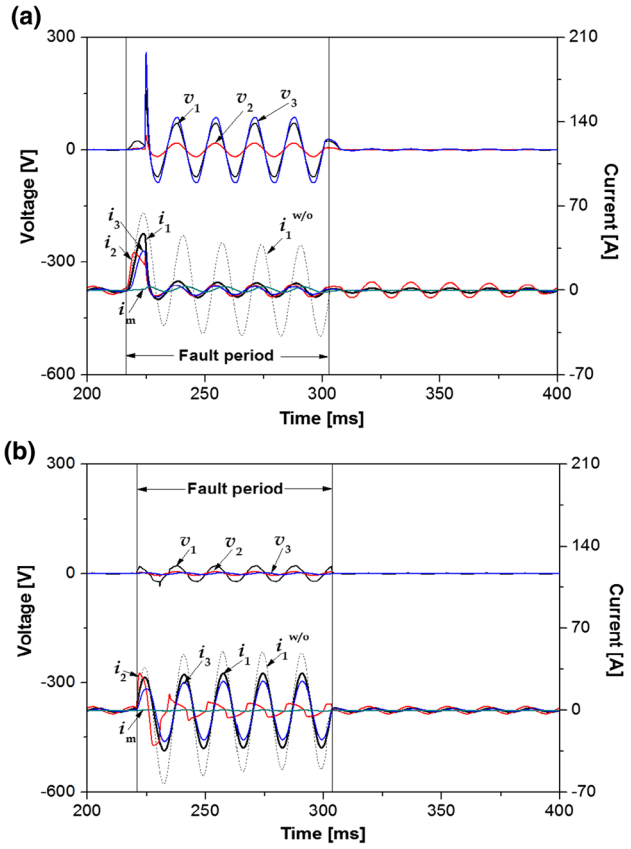

Fig. 4 Current limiting characteristics and voltage waveform in each winding of the transformer type SFCL in case of the fault angle at **a** 0° and **b** 90°

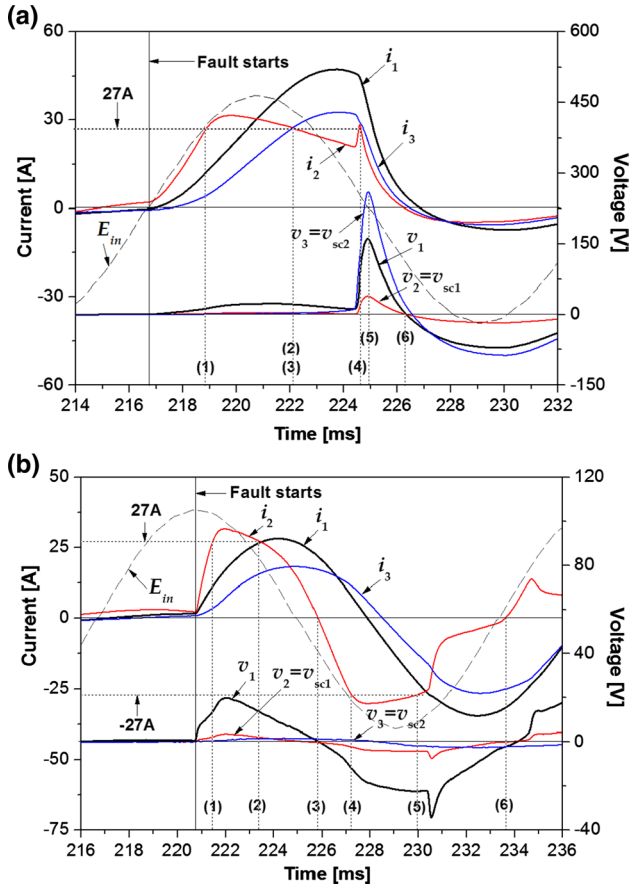

Fig. 5 Transient fault current limiting characteristics and voltage waveform in each winding of the transformer type SFCL in case of the fault angle at **a** 0° and **b** 90°

occurs in superconducting element SC_1 constituting the first limiting element while the quench does not occur in superconducting element SC_2 constituting the second limiting element. Therefore, it can be seen that the total current of the SFCL is initially small when the fault occurs, and then the total current increases It is shown that superconducting element SC_2 constituting the second limiting element is not quenched, but only the fault current is limited by the quench of superconducting element SC_1 constituting the first limiting element. In addition, it can be seen that the current (i_2) flowing in the superconducting element SC_1 is distorted.

Figure 5(a) shows the operation characteristics according to the transient component of the fault current at a fault angle of 0°. The current and voltage of the superconducting elements connected to the secondary winding and the tertiary winding when the fault occurs are shown. Immediately after the fault's occurrence, it can be seen that the fault current is limited by the generation of the quench of superconducting elements SC_1 and SC_2 constituting the first and second limiting elements. It can be seen that the voltages (v_{sc1} and v_{sc2}) of the superconducting elements are induced after a 1/2 cycle.

Figure 5(b) shows the operation characteristics according to the transient component of the fault current at the fault angle of 90°. Immediately after the occurrence of the fault, the voltage of superconducting element SC_1 appears due to the generation of the quench of superconducting element SC_1 constituting the first limiting element. It can be seen that the voltage of superconducting element SC_1 is generated again when the critical current is exceeded after a 1/2 cycle. Superconducting element SC_2 constituting the second limiting element exhibits zero voltage without being quenched due to a small fault current.

Figure 6 shows the relationship between the instantaneous power consumed by each element and the magnetic flux of the transformer type SFCL with two isolated secondary windings according to the fault angle immediately after the fault. The instantaneous power and magnetic flux consumed at the fault angle of 0° are shown in Fig. 6(a). Since the quench occurred in superconducting elements SC_1 and SC_2, which constitute the first and second limiting elements, the power consumption and magnetic flux are larger than when the fault angle is 90°. As shown in Fig. 6(b), when the fault

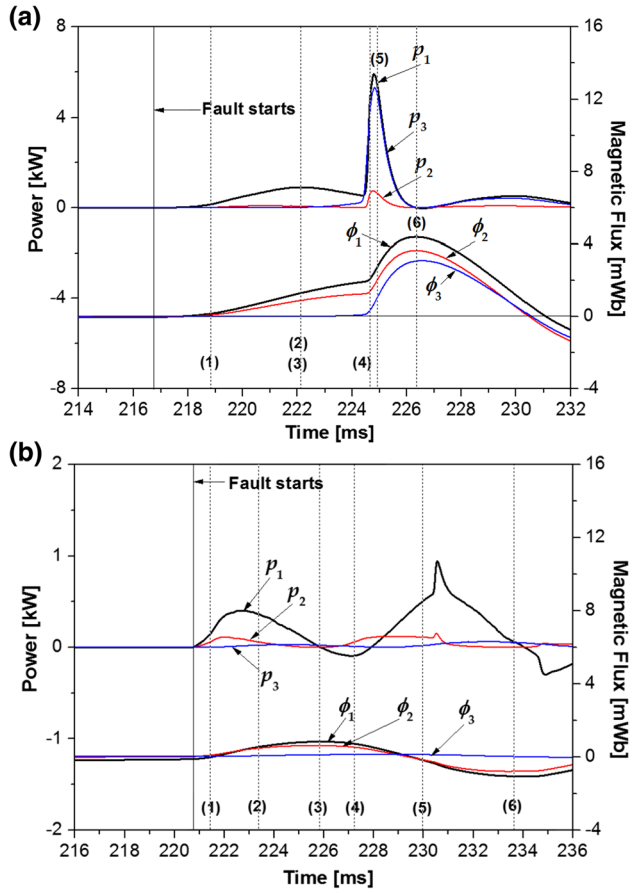

Fig. 6 Instantaneous powers and magnetic flux in each winding of the transformer type SFCL in case of the fault angle at **a** 0° and **b** 90°

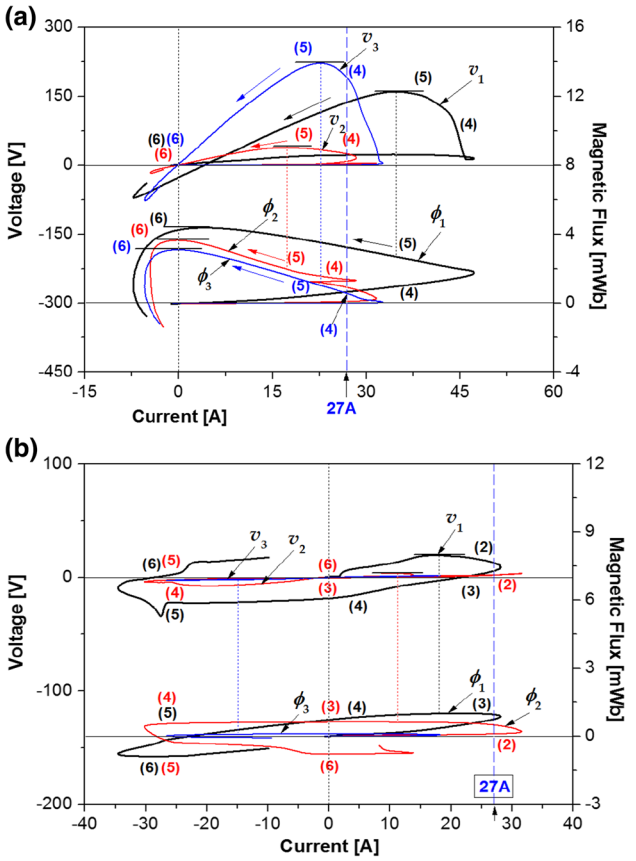

Fig. 7 Variation in voltage and magnetic flux depending on the current flowing in each winding during one fault period of the transformer type SFCL in case of the fault angle at **a** 0° and **b** 90°

angle is increased to 90°, the power consumption and magnetic flux of superconducting element SC_1 and the primary winding are small. It can be seen that the power consumption and magnetic flux are zero because no quench occurs in superconducting element SC_2 constituting the second limiting element.

Figure 7 shows the voltage and magnetic flux fluctuation area of each SFCL element depending on the current of the transformer type SFCL with two insulated secondary windings based on the fault angle immediately after the fault. As shown in Fig. 7(a), the maximum voltage value of superconducting element SC_2 depending on the current at the fault angle of 0° was 222.52 V. The maximum voltages of the primary winding and superconducting element SC_1 were 162.38 V and 39.46 V, respectively. Immediately after the fault, the magnitude of the magnetic flux fluctuation region depending on the current flowing through each element of the SFCL was the largest in the magnetic flux (ϕ_1) generated in the primary winding, followed by the magnetic flux (ϕ_2) generated in the secondary winding. In addition, the magnetic flux (ϕ_3) generated in the tertiary winding was the smallest.

Figure 7(b) shows that the maximum voltage value of the primary winding is 19.51 V depending on the current at the fault angle of 90°. The maximum voltage values of superconducting elements SC_1 and SC_2 are -7.61 V and 0 V, respectively. Immediately after the fault, the magnitude of the magnetic flux fluctuation region depending on the current flowing through each element of the SFCL was the largest in the magnetic flux (ϕ_1) generated in the primary winding, followed by the magnetic flux (ϕ_2) generated in the secondary winding. The magnetic flux (ϕ_3) generated in the tertiary winding was the smallest.

Figure 8 shows the power consumption and energy consumption characteristics of the SFCL elements depending on the current during one fault period of the transformer type SFCL with two isolated secondary windings according to the fault angle. As shown in Fig. 8(a), the maximum power consumption of superconducting elements SC_1 and SC_2, and primary windings depending on the current during one fault period at the fault angle of 0° is 0.78 kW, 5.32 kW, and 5.94 kW, respectively. In addition, the energy consumption of this transformer type SFCL was the largest in the primary winding and the smallest in superconducting element SC_1.

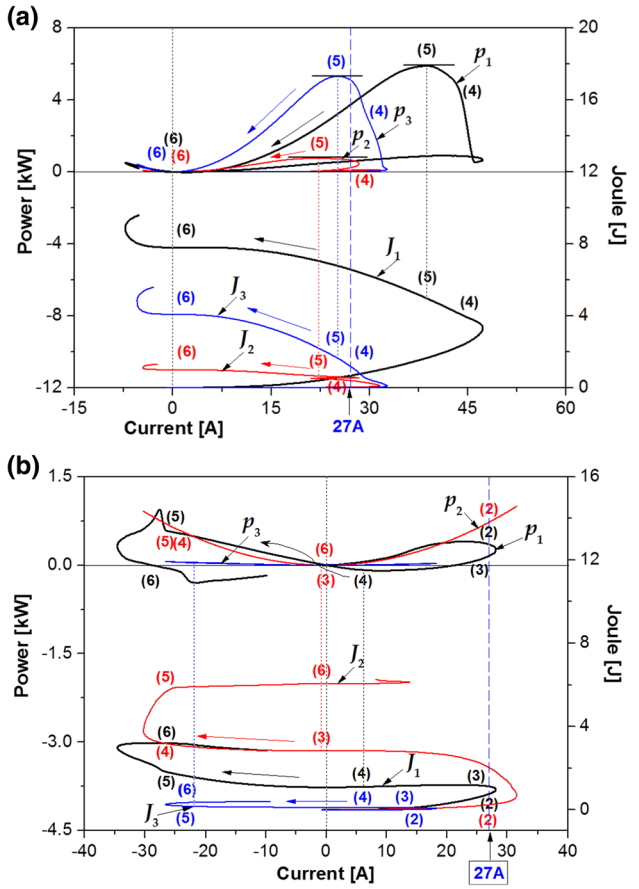

Fig. 8 Characteristics of power consumption and energy consumption according to the current flowing in each winding during one fault period of the transformer type SFCL in case of the fault angle at **a** 0° and **b** 90°

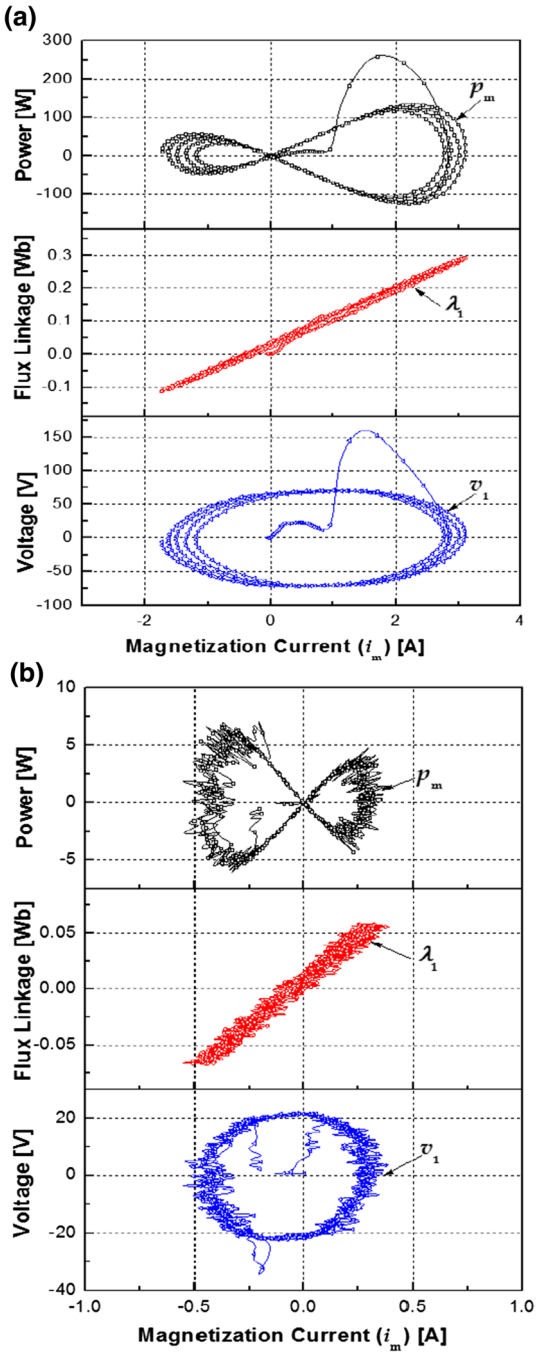

Fig. 9 Variation of magnetization force (p_m), flux linkage's (λ) operating range, and voltage (v_1) according to the magnetization current (i_m) during five fault periods of the transformer type SFCL in the case of the fault angle at **a** 0° and **b** 90°

Figure 8(b) shows the power consumption and energy consumption of the SFCL elements depending on the current during one fault period at the fault angle of 90°. During one fault period, the power consumption at the primary winding and superconducting elements SC_1 and SC_2 were both much lower than at the fault angle of 0°. The energy consumption was the highest in superconducting element SC_1 and the smallest in the primary winding and superconducting element SC_2. Although the energy consumption of the superconducting element SC_1 was higher than that of the fault angle 0°, the energy consumption of superconducting element SC_2 was lower than that of the fault angle of 0°.

Figure 9 shows the variation of the magnetization force, the operating range of the flux linkage, and the voltage range change depending on the magnetization current of the transformer type SFCL with two insulated secondary windings at the fault angles of 0° and 90° during the five fault period. In order to analyze the magnetic energy that accumulated in the ferromagnetic iron core, the change in the magnetization force (p_m), which can be derived from the product of the magnetization current (i_m) and the magnetization branch voltage, was displayed from one to five cycles of failure at the fault angle of 0°.

From the comparison of the change in the magnetization force according to the fault angle, it can be observed that the change in the magnetization force at the fault angle of

0° was much larger than that at the fault angle of 90°. The flux linkage (λ) induced in the magnetization branch can be obtained by integrating the voltage (v_1) induced in the primary winding of the SFCL. For five cycles of failure, it can be observed that the operating range of the flux linkage dependent on the magnetization current at the fault angle of 0° was about six times greater than at the fault angle of 90°. Due to the large transient fault current, the magnetization current became larger, which was expected to accumulate more magnetic energy in the ferromagnetic iron core. From the comparison of the region change of voltage (v_1) induced by the magnetization current in the primary winding at the fault angles of 0° and 90°, it can be seen that the change of the region of v_1 at the fault angle of 0° was about three times larger than that of the fault angle of 90°. It is shown that the voltage induced in the primary winding through the ferromagnetic iron core by the magnetization current was stabilized by drawing an ellipse for five cycles of failure due to the increase or decrease of the magnetization current. As a future study, magnetic field analysis using COMSOL MULTIPHYSICS tool to evaluate AC loss of superconducting elements and modeling analysis of iron loss of transformer type SFCL will be performed.

4 Conclusion

In this paper, to increase the current limiting capacity, the magnetization characteristics of a transformer type SFCL insulated by secondary and tertiary windings on the secondary side of the transformer were compared at fault angles of 0° and 90°. From the results, the double quench occurred in the superconducting elements SC_1 and SC_2 at the fault angle of 0°, but quench only occurred in superconducting element SC_1 at the fault angle of 90°. During the five cycles of failure, the magnetization current was larger in the case of the fault angle of 0° than in the case of the fault angle of 90°. The quench occurred in superconducting elements SC_1 and SC_2 constituting the first and second limiting elements, and thus the power consumption and the magnetic flux were larger when the fault angle was 0° than when the fault angle was 90°. It was observed that the magnetization force change was much greater in the case of the fault angle of 0° than in the case of the fault angle of 90°. It was observed that the operating range of the flux linkage at the fault angle of 0° was about six times larger than that at the fault angle of 90°. The change in the voltage (v_1) region induced in the primary winding due to the magnetization current confirmed that the fault angle of 0° was three times greater than the fault angle of 90°. In the future, a basic study will be conducted on whether this modified bridge type SFCL model can be applied to a DC power distribution system.

Acknowledgements This research was supported by Basic Science Research Program through the National Research Foundation of Korea (NRF) funded by the Ministry of education (2018R1D1A1B07040471) and funded by the Ministry of education (2018R1D1A1B09083558).

References

1. Noe M, Steurer M (2007) High-temperature superconductor fault current limiters: Concepts, applications, and development status. Supercond Sci Technol 20(3):R15–R29
2. Barzegar-Bafrooei M, Foroud A, Ashkezari J, Niasati M (2019) On the advance of SFCL: a comprehensive review. IET Gener Transm Distrib 13(17):3745–3759
3. Wheeler K, Elsamahy M, Faried S (2017) Use of superconducting fault current limiters for mitigation of distributed generation influences in radial distribution network fuse-recloser protection systems. IET Gener Transm Distrib 11(7):1605–1612
4. Neumueller HW et al (2009) Development of resistive fault current limiters based on YBCO coated conductors. IEEE Trans Appl Supercond 19(3):1950–1955
5. Xin Y et al (2009) Manufacturing and test of a 35 kV/90 MVA saturated iron-core type superconductive fault current limiter for live-grid operation. IEEE Trans Appl Supercond 19(3):1934–1937
6. Hekmati (2015) Multi-objective design of tunable shield-type superconducting fault current limiter. IEEE Trans Appl Supercond 25(5):5602908
7. Salim KM, Hoshino T, Kawasaki A, Muta I, Nakamura T (2003) Waveform analysis of the bridge type SFCL during load changing and fault time. IEEE Trans Appl Supercond 13(2):1992–1995
8. Ko SC, Han TH, Lim SH (2020) Magnetizing characteristics of bridge type superconducting fault current limiter (SFCL) with simultaneous quench using flux-coupling. Energies 13(7):1760
9. Hyun OB, Sim J, Kim HR, Park KB, Yim SW, Oh IS (2009) Reliability enhancement of the fast switch in a hybrid superconducting fault current limiter by using power electronic switches. IEEE Trans Appl Supercond 19(3):1843–1846
10. Lee GH et al (2009) Hybrid superconducting fault current limiter of the first half cycle non-limiting type. IEEE Trans Appl Supercond 19(3):1888–1891
11. Choi HS, Lim SH (2007) Operating performance of the flux-lock and the transformer type superconducting fault current limiter using the YBCO thin films. IEEE Trans Appl Supercond 17(2):1823–1826
12. Lim SH, Moon JF, Kim JC (2009) Improvement on current limiting characteristics of a flux-lock type SFCL using E-I core. IEEE Trans Appl Supercond 19(3):1904–1907
13. Ren L et al (2010) Techno-economic evaluation of a novel flux-coupling type superconducting fault current limiter. IEEE Trans Appl Supercond 20(3):1242–1245
14. Yan S et al (2018) Electromagnetic design and performance analysis of a flux-coupling-type SFCL. IEEE Trans Appl Supercond 28(3):5600305
15. Lee BW, Park KB, Sim J (2018) Design and experiments of novel hybrid type superconducting fault current limiters. IEEE Trans Appl Supercond 18(2):624–627
16. Ko SC, Han TH, Lim SH (2014) Analysis on current limiting characteristics according to the influence of the magnetic flux for SFCL with two magnetic paths. J Elect Eng Technol 9(6):1909–1913
17. Lim SH, Kim YP, Ko SC (2016) Effect of peak current limiting in series-connection SFCL with two magnetically coupled circuits using E-I core. IEEE Trans Appl Supercond 26(3):5600404

18. Yu B, Han TH, Lim SH, Kim YP, Ko SC (2018) Comparison of dual peak current limiting operation for a series-connected SFCL using two iron cores. IEEE Trans Appl Supercond 28(4):5600704
19. Han TH, Ko SC, Lim SH (2018) Fault current limiting characteristics of transformer-type superconducting fault current limiter due to winding direction of additional circuit. IEEE Trans Appl Supercond 28(3):5601906
20. Han TH, Ko SC, Lim SH (2018) Peak current limiting characteristics of transformer type superconducting fault current limiters with two non-isolated secondary windings. IEEE Trans Appl Supercond 28(4):5603205
21. Ko SC, Lim SH (2016) Analysis on magnetizing characteristics due to peak fault current limiting operation of a modified flux-lock-type SFCL with two magnetic paths. IEEE Trans Appl Supercond 26(4):5601605

Tae-Hee Han He received his B.S., M.S., and Ph.D. degrees from Chonbuk National Univ., Korea in 1991, 1994, and 1999, respectively. ππCurrently, he is a professor in the Dept. of Aero Materials Engineering at Jungwon Univ., Korea.

Sung-Hun Lim He received his B.S., M.S., and Ph.D. degrees from Chonbuk National Univ., Korea in 1996, 1998, and 2003, respectively. Currently, he is a professor in the Dept. of Electrical Engineering at Soongsil Univ., Korea.

Seok-Cheol Ko He received his B.S., M.S., and Ph.D. degrees from Chonbuk National Univ., Korea in 1996, 2002, and 2005, respectively. Currently, he is a professor in the Industry-University Cooperation Foundation at Kongju National Univ., Korea.